Supplementary Information

Morphology Evolution of Fcc Ru Nanoparticle under Hydrogen Atmosphere

Lili Liu[a,b], Mengting Yu[a,b], Bo Hou[a], Qiang Wang[a,*], Beien Zhu[c,*], Litao Jia[a,d] and Debao Li[a,d,*]

[a] *State Key Laboratory of Coal Conversion, Institute of Coal Chemistry, Chinese Academy of Sciences, Taiyuan, Shanxi 030001, China*

[b] *University of Chinese Academy of Sciences, Beijing 100049, China*

c Shanghai Advanced Research Institute, Chinese Academy of Sciences, Shanghai, 201210 China

[d] *Dalian National Laboratory for Clean Energy, Dalian 116023, China*

[*] Corresponding author, E-mail address: wqiang@sxicc.ac.cn (Qiang Wang), zhubeien@sinap.ac.cn (Beien Zhu) and dbli@sxicc.ac.cn (Debao Li)

Content

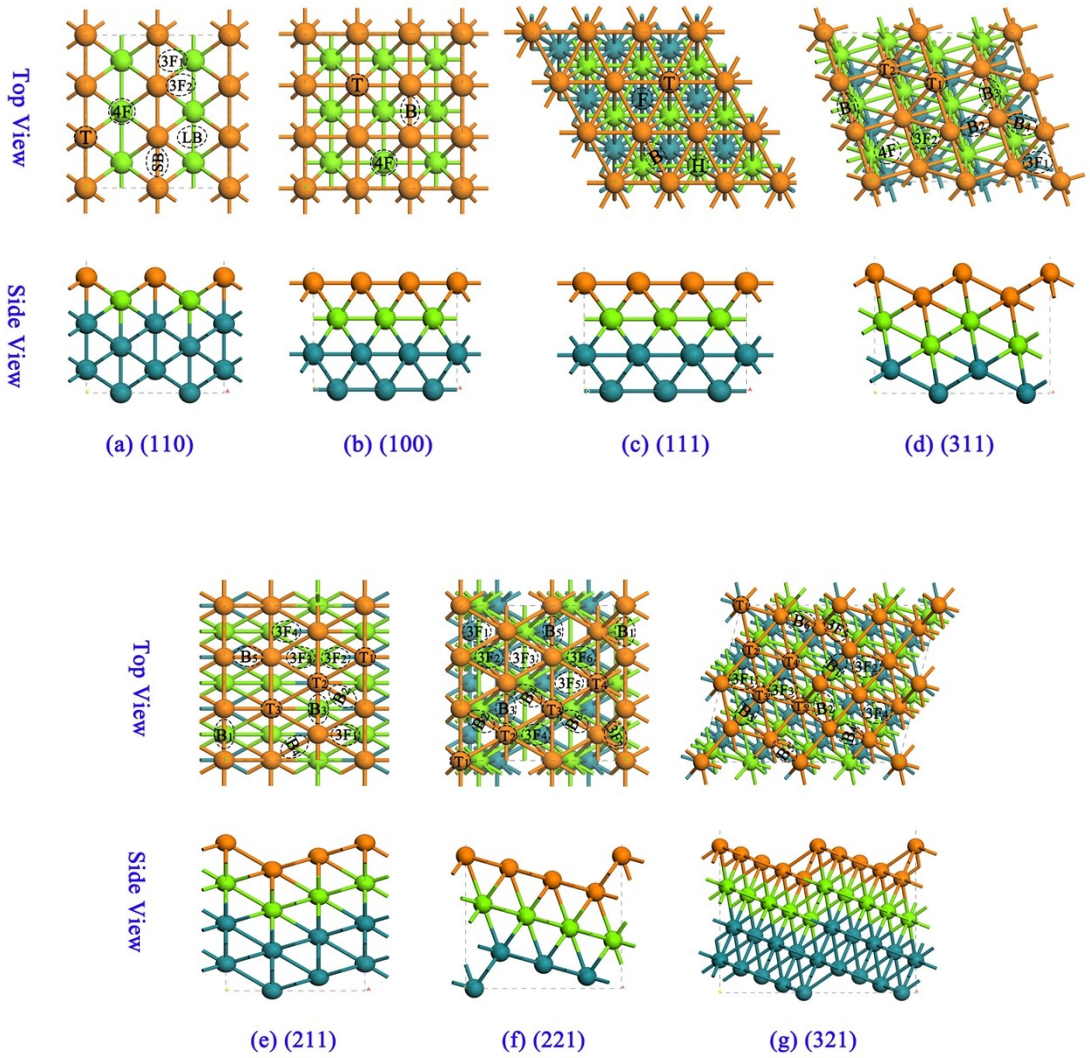

Fig. S1 Top and side view of (a) Ru(110), (b) Ru(100), (c) Ru(111), (d) Ru(311), (e) Ru(211), (f) Ru(221) and (g) Ru(321) surfaces. All possible adsorption sites are indicated in the top figures (see text for more information). The Ru surface atoms (top layer and second layer) are colored by orange and light green, respectively, and dark green for layers below.

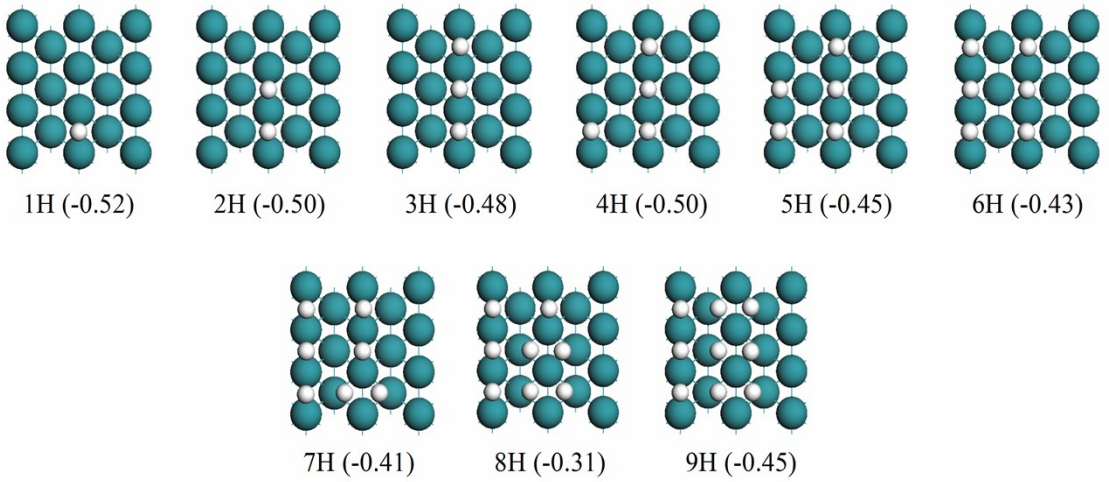

Fig. S2 Stable adsorption configurations and corresponding stepwise adsorption energies (eV) of hydrogen at different coverage on Ru(110) surface. The Ru atoms and adsorbed H atoms are colored dark green and white, respectively.

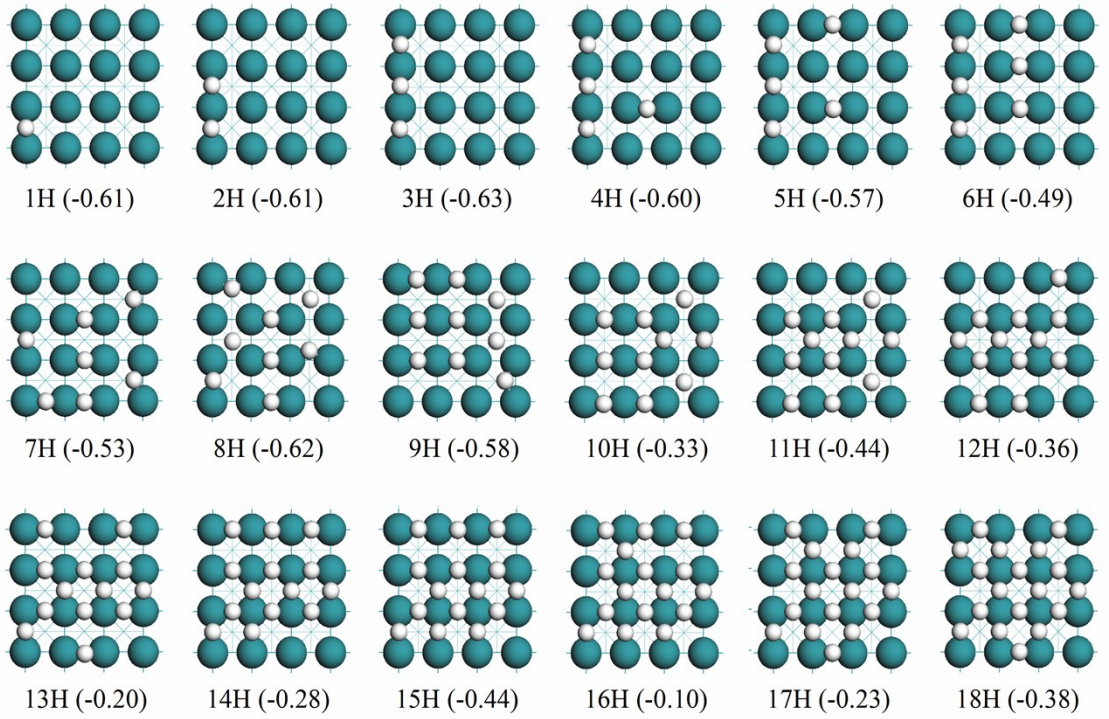

Fig. S3 Stable adsorption configurations and corresponding stepwise adsorption energies (eV) of hydrogen at different coverage on Ru(100) surface. The Ru atoms and adsorbed H atoms are colored dark green and white, respectively.

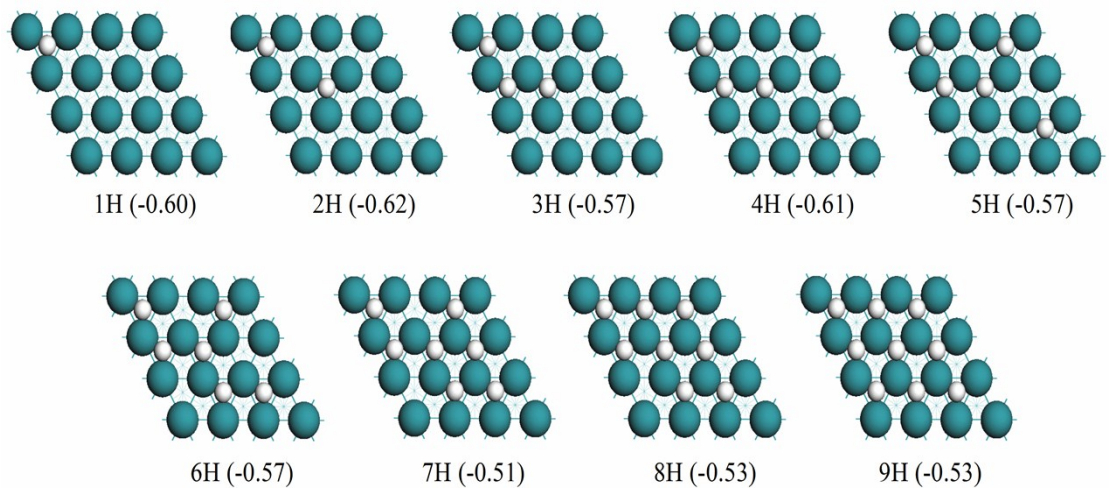

Fig. S4 Stable adsorption configurations and corresponding stepwise adsorption energies (eV) of hydrogen at different coverage on Ru(111) surface. The Ru atoms and adsorbed H atoms are colored dark green and white, respectively.

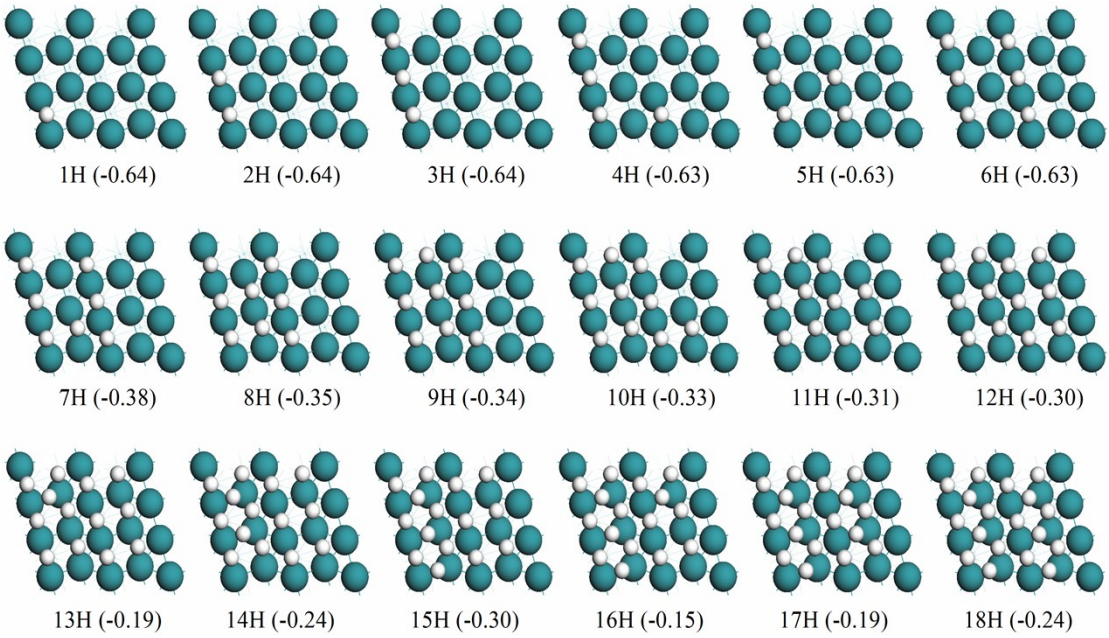

Fig. S5 Stable adsorption configurations and corresponding stepwise adsorption energies (eV) of hydrogen at different coverage on Ru(311) surface. The Ru atoms and adsorbed H atoms are colored dark green and white, respectively.

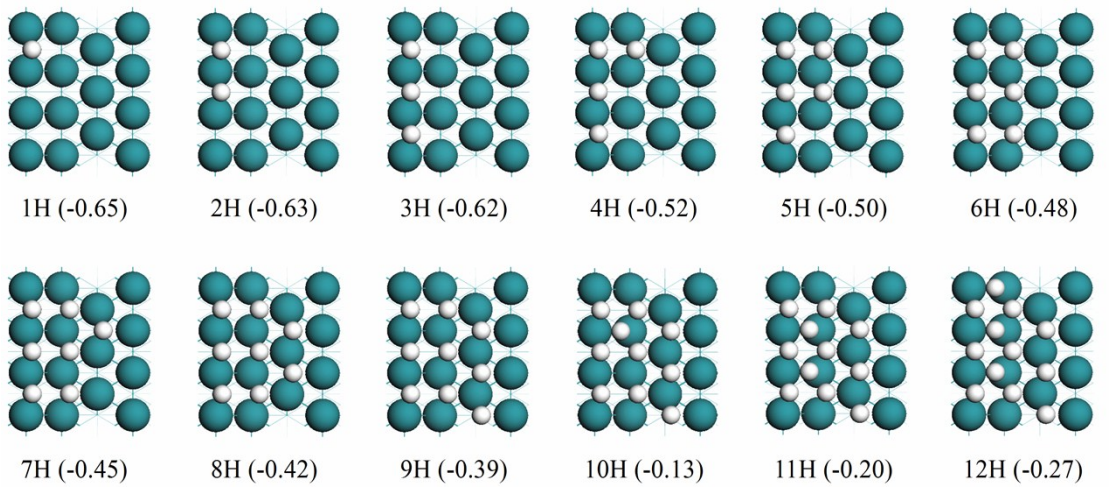

Fig. S6 Stable adsorption configurations and corresponding stepwise adsorption energies (eV) of hydrogen at different coverage on Ru(211) surface. The Ru atoms and adsorbed H atoms are colored dark green and white, respectively.

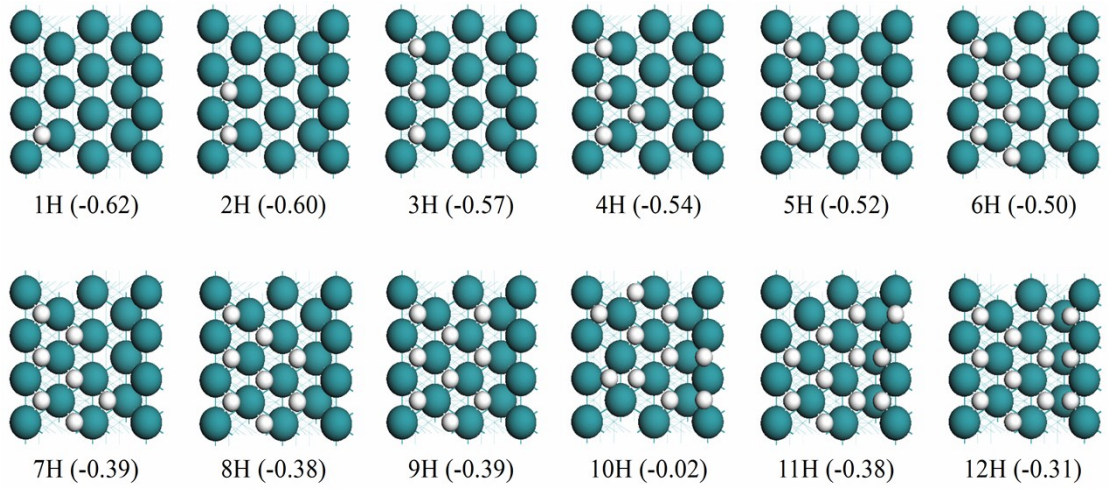

Fig. S7 Stable adsorption configurations and corresponding stepwise adsorption energies (eV) of hydrogen at different coverage on Ru(221) surface. The Ru atoms and adsorbed H atoms are colored dark green and white, respectively.

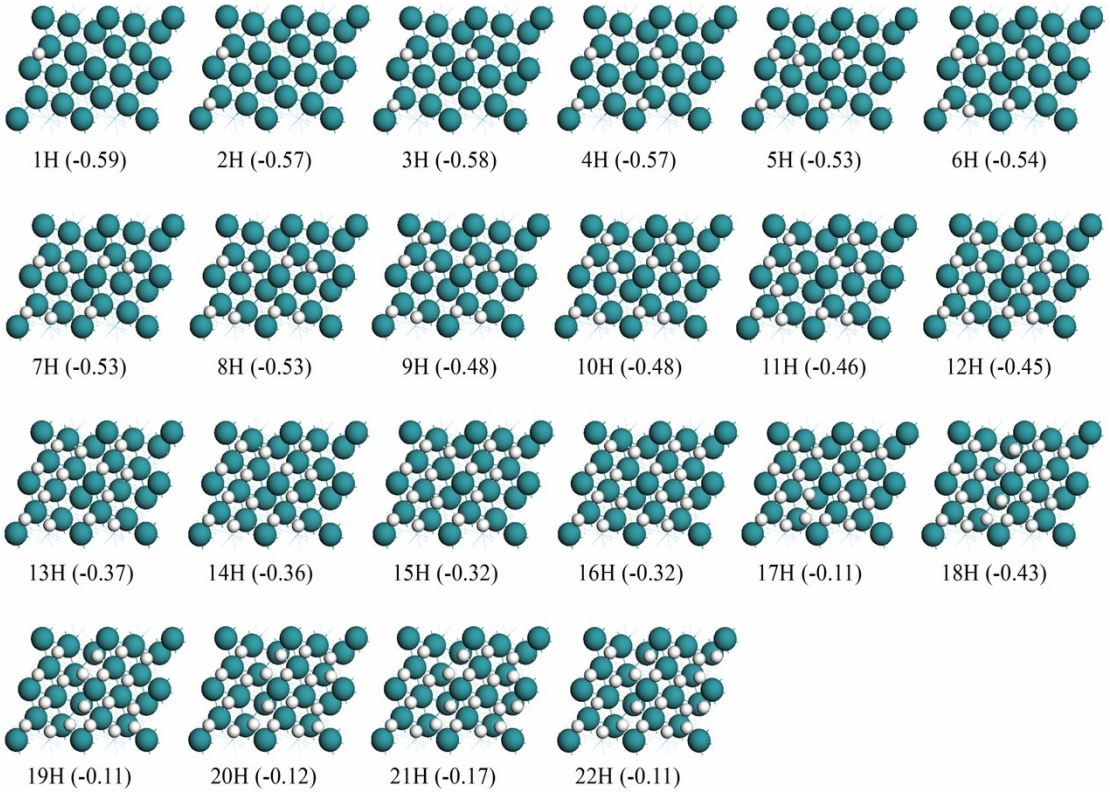

Fig. S8 Stable adsorption configurations and corresponding stepwise adsorption energies (eV) of hydrogen at different coverage on Ru(321) surface. The Ru atoms and adsorbed H atoms are colored dark green and white, respectively.

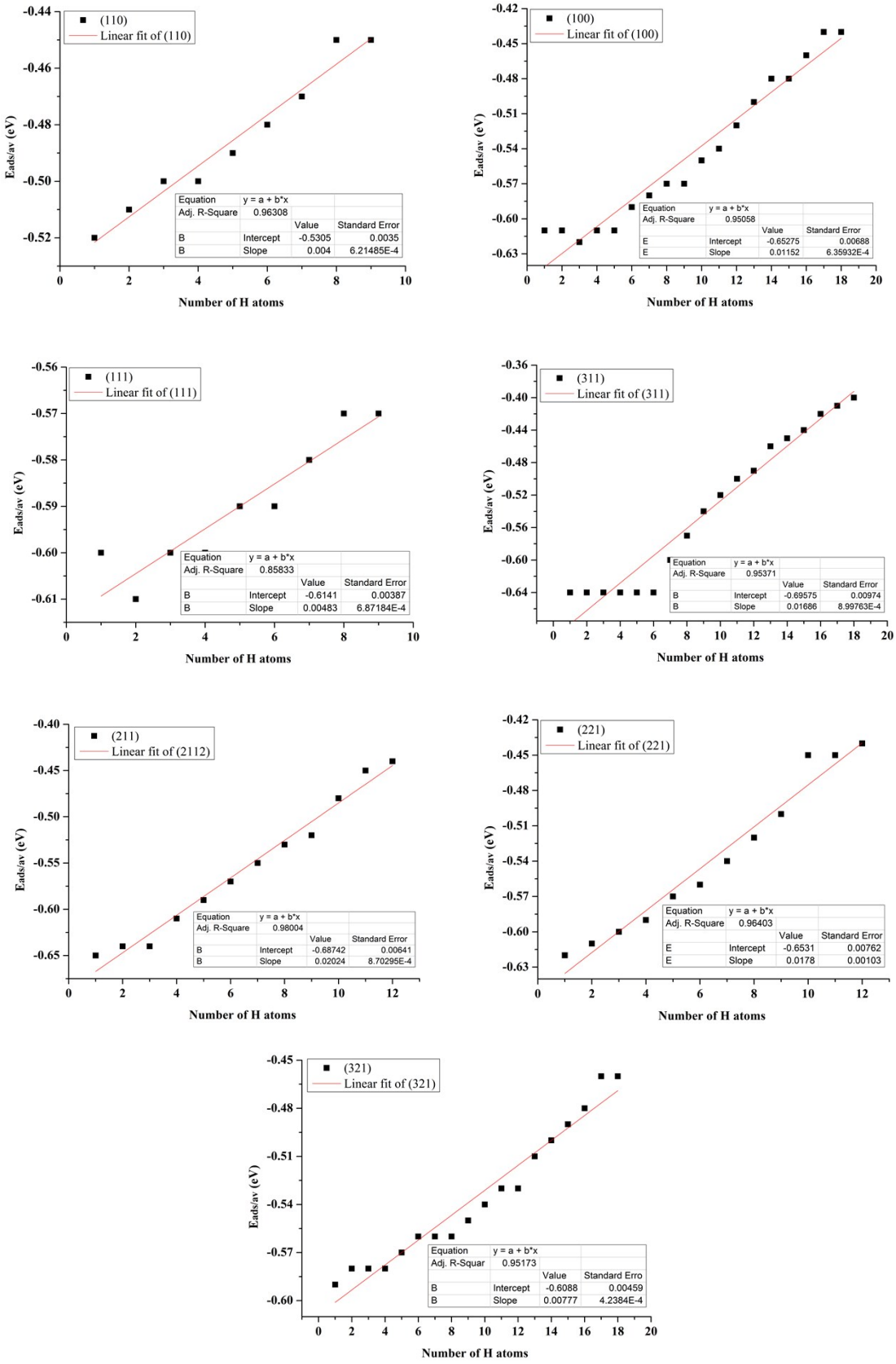

Fig. S9 Fitted parameters and curves of the fitted lateral interaction energy between the adsorbed H atoms on each Ru surfaces.

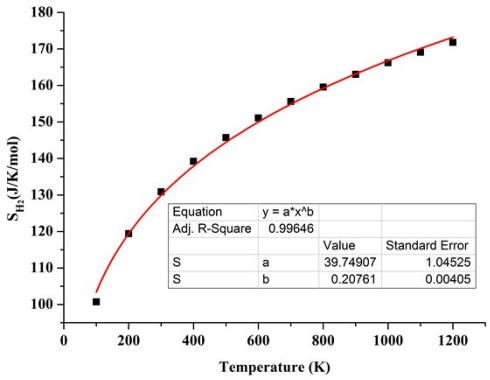

Fig. S10 Fitted parameters and curves of the entropies of gas-phase H_2. The fitting data are from NIST-JANAF Thermochemical TABLEs (http://kinetics.nist.gov/janaf/).

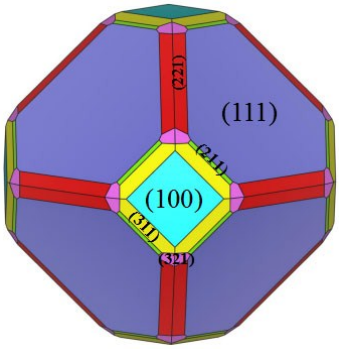

Fig. S11 Equilibrium shape of fcc Ru nanoparticles in vacuum obtained by Wulff construction.

To elucidate the nature of the hydrogenation abilities in terms of the interaction between Ru surfaces and adsorbed H atoms, the projected density of states (PDOS) onto Ru d-orbitals of clean surfaces and adsorption systems as well as H s orbitals of saturation adsorption were calculated and illustrated in Fig. S12. The electronic states occupied by Ru d orbitals of seven clean Ru surfaces are distinct from each other (Fig. S12a), implying their different intrinsic surface structures. And the various sharp peaks of the Ru d orbitals near the Fermi level for seven Ru surfaces also reveal a significant difference in their active sites and hydrogen adsorption strength. Upon hydrogen adsorption to saturation, these Ru d orbitals have a downward shift (Fig. S12b), leading to the hybridization with the H s orbitals. In comparison, it is noted that there are more overlaps between H s-states and Ru d-states in Ru(100), Ru(311) and Ru(321) adsorption systems, resulting from the stronger H adsorption. Generally, our results show that the interaction between H atoms and Ru surfaces is reflected in the hybridization of Ru d orbitals with the H s orbitals below Fermi level, which in turn indicates the relative hydrogenation abilities of different Ru surfaces.

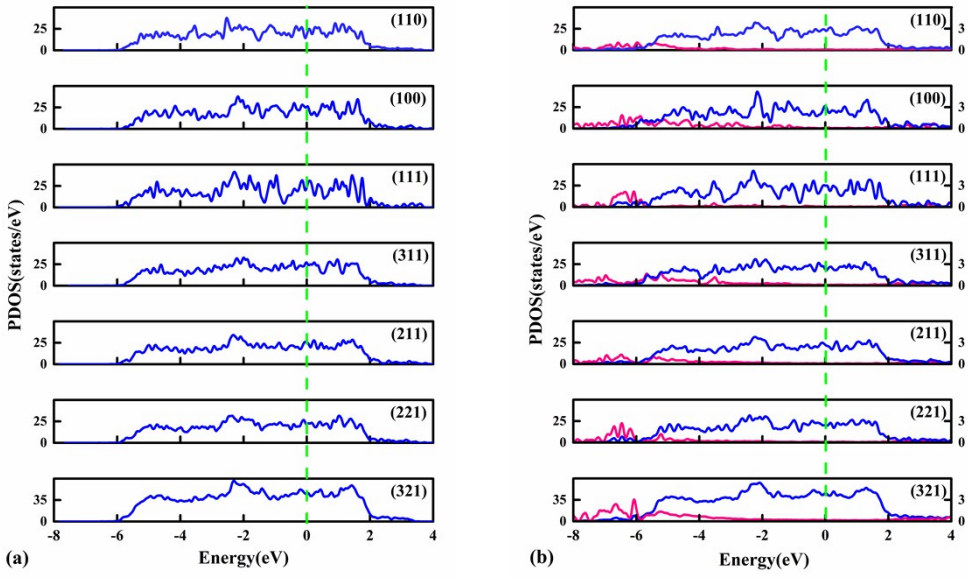

Fig. S12 The projected density of states (PDOS) onto Ru d-orbitals for the seven (a) clean Ru surfaces and (b) Ru surfaces with saturated adsorbed H. The projected density of states onto s-orbitals of adsorbed H atoms at saturation coverage are also depicted in (b). The Ru atoms are shown in blue and H atoms are shown in pink.

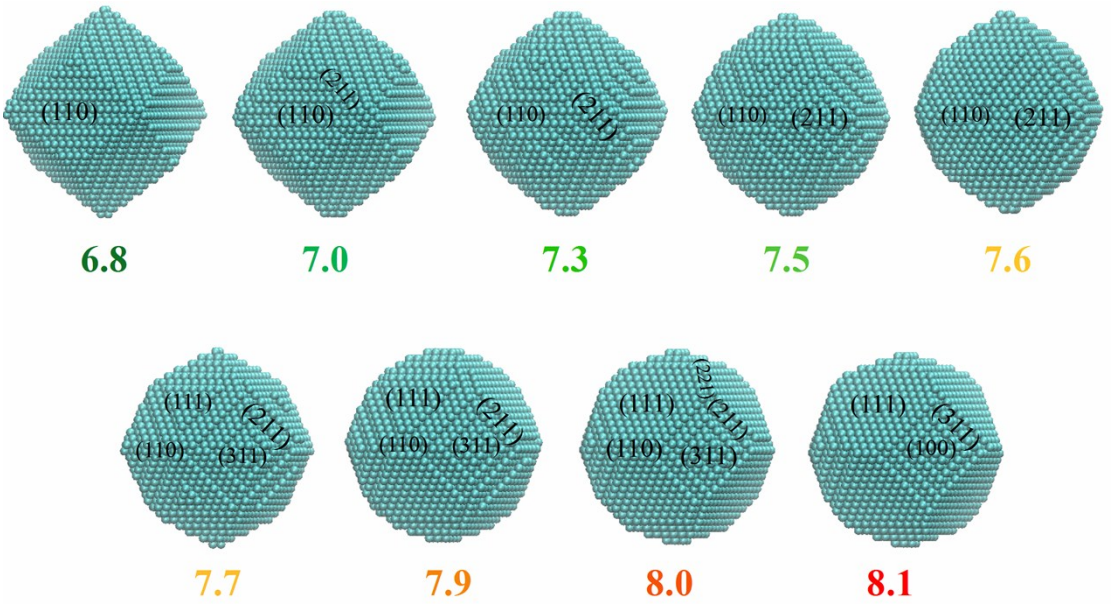

Fig. S13 Full sets of constructed structures of Ru NPs with 5 nm diameters under H_2 conditions. Color mapped $\overline{CN}$ is marked below.

Table S1 Calculated surface energies (eV/Å^2) with corresponding coordination number $\overline{CN}$ on different facets of fcc Ru based on the Wulff construction.

Facet	Surface energy (eV/Å^2) with coordination number $\overline{CN}$					
	6.8	7.0	7.5	7.7	8.0	8.1
(110)	0.016	0.024	0.041	0.110	0.133	0.174
(100)	0.102	0.117	0.133	0.156	0.161	0.166
(111)	0.047	0.052	0.061	0.104	0.117	0.140
(311)	0.049	0.053	0.063	0.110	0.127	0.157
(211)	0.022	0.027	0.039	0.101	0.124	0.173
(221)	0.035	0.042	0.054	0.110	0.129	0.166
(321)	0.054	0.061	0.074	0.128	0.143	0.169

Table S2. The surface fraction of exposed facets under different conditions.

$\overline{CN}$	Area proportion of exposed facets						
	(110)	(100)	(111)	(311)	(211)	(221)	(321)
6.8	100%	0.0%	0.0%	0.0%	0.0%	0.0%	0.0%
7.0	82.8%	0.0%	0.0%	0.0%	17.2%	0.0%	0.0%
7.5	11.3%	0.0%	0.0%	0.0%	88.7%	0.0%	0.0%
7.7	4.5%	0.0%	2.2%	1.4%	91.9%	0.0%	0.0%
8.0	5.6%	0.0%	29.9%	29.6%	32.4%	2.5%	0.0%
8.1	0.0%	1.9%	56.8%	41.3%	0.0%	0.0%	0.0%